GT2019-92058

Thermal Characterization of a Turbulent Free Jet with Planar Laser Induced Fluorescence (PLIF)

Sara Seitz¹ and Lesley M. Wright²

¹Baylor University Department of Mechanical Engineering Waco, Texas 76798-7356 ²Texas A&M University
Department of Mechanical Engineering
College Station, Texas 77843-3123
Lesley_Wright@TAMU.edu

ABSTRACT

Two-color, toluene based, planar laser induced fluorescence (PLIF) is utilized to characterize the thermal structure of a turbulent, free jet. The PLIF technique has been used to measure concentration gradients for combustion applications, but its use to quantify thermal gradients is limited. To validate the method, compressed air is seeded with toluene particles. The seeded airflow is heated to temperatures varying from 300 – 375 K, and the heated jet exits a 1.27-cm diameter orifice into quiescent, room temperature air. The jet Reynolds number is varied from 5,000 to 15,000. As the jet exits the orifice, the toluene particles fluorescence across a 266 nm laser light sheet which ultimately provides a two-dimensional temperature distribution of the free jet. The rigorous calibration procedure for the PLIF technique is described along with the seeding nuisances needed to quantify the thermal structure of the jets. The PLIF technique has been demonstrated for this fundamental flow field, and it has proven to be applicable to more complex heat transfer and cooling applications. Furthermore, the time averaged temperature distributions obtained in this investigation can be used in the validation of turbulent CFD solvers.

NOMENCLATURE

NOMENOLATORE				
Constant representing the thermal, streamwise length				
scale (similarity solution)				
Speed of light in a vacuum				
Nozzle (jet) diameter				
Laser energy				
Focal length				
Spectral transmission curve				
Temperature independent spectral transmission curve				
Temperature dependent spectral transmission curve				
Planck's constant				
Intensity				
Temperature independent fluorescence intensity of				
background images				

$I_{Back\text{-}Red}$	Temperature dependent fluorescence intensity of
7	background images
I_{Blue}	Temperature independent fluorescence intensity of
7	toluene / air images
I_N	Normalized fluorescence intensity of toluene / air images
I_{Red}	Temperature dependent fluorescence intensity of
7	toluene / air images
I_{Ref}	Intensity ratio at reference temperature
n_i	Spectral response of optical system
$n_{i ext{-}Blue}$	Temperature independent spectral response of optical
	system
$n_{i\text{-}Red}$	Temperature dependent spectral response of optical
	system
R	Radial coordinate (from jet center)
Re	Jet Reynolds number $(\rho VD/\mu)$
S_{f}	Fluorescence signal
$S_{f ext{-}Blue}$	Temperature independent fluorescence signal
$S_{f ext{-}Red}$	Temperature dependent fluorescence signal
T	Temperature
T_{Jet}	Jet temperature (outlet of nozzle)
T_{PLIF}	Temperature measured at the exit of the nozzle using PLIF
T_{Ref}	Reference (room) temperature
T_{TC}	Temperature measured at the exit of the nozzle using
	thermocouples
V	Jet velocity
Z	Axial coordinate (along jet centerline)
ϕ	Fluorescence quantum yield
η_{tol}	Tracer number density
λ	Wavelength of excitation laser
μ	Dynamic viscosity
θ	Non-dimensional temperature
ρ	Density
\sim	Delibity

INTRODUCTION

Absorption cross-section

Experimental methods are important for analyzing heat transfer surfaces and thermal flow fields. Having a better

understanding of the temperature distribution within the flow field, and over the surface (through thermal boundary layer), leads to improved system performance. Several experimental methods have been developed to obtain measurements of a surface temperature. Characterizing the boundary layer has always been a challenge. Using a direct method to measure the temperature, such as thermocouples, interrupts the flow structure. Thus, there is a need to develop a nonintrusive method to measure the temperature gradient within the boundary layer.

Surface visualization methods have recently become very popular for surface heat transfer measurements [1, 2]. In addition to surface thermal characterization, it is also crucial to characterize the flow behavior above the surface especially within the thermal boundary layer. Planar Laser Induced Fluorescence (PLIF) could be a solution to this challenge by providing a quantitative relationship between the fluid temperature and fluorescence intensity [3].

PLIF is a two-dimensional, non-intrusive, optical diagnostic method with a potential to measure the flow field parameters such as concentration and temperature. PLIF has been widely used to measure the concentration, particularly in many combustion studies [4, 5]. The purpose of this study is to develop a novel PLIF-based technique. While the current work applies this PLIF method to a heated, free jet, the opportunity exists to apply the method to near wall flows to quantify thermal boundary layer development. Having the capacity to measure the near wall temperature profile provides unparalleled insight into convective heat transfer. This method has the potential to be used in other applications that require the knowledge of fluid temperature gradients. In addition, with the application of this process to highly turbulent flows (as seen in gas turbine cooling applications), the results can also be used to validate state - of - the - art computational fluid dynamics models.

PLIF History

Laser induced fluorescence (LIF) has made significant contributions towards flow visualization, quantification, particularity, and concentration characterization. Long et al. [6] initially demonstrated planar visualization based on Laser Rayleigh Scattering for concentration measurements within turbulent jets in the late 1970's. A short time later, in 1982, linear and planar imaging using hydroxide-LIF was presented. Kychakoff et al. [7] applied linear LIF for concentration measurement of hydroxide within combustion gases. Additionally, Dyer and Crosley [8] mapped the hydroxide concentration using planar laser induced fluorescence (PLIF). In 1985, Allen and Hanson [9] used PLIF for vapor and liquid visualization in fuel spray. McDaniel et al. [10] also used PLIF to measure the velocity distribution within a plane of gaseous flow using iodine-PLIF. In the same year, Seitzman et al. [11] proposed nitrogen oxide-PLIF for quantitative temperature visualization in combustion flows.

Technical improvements in optical systems such as cameras, filters, and lenses have assisted in allowing PLIF diagnostics for other parameters, particularly, temperature measurements. In 1999, Thurber [12] studied the fluorescence dependency of acetone aimed to make PLIF more applicable for quantitative temperature measurements. Shortly after that, Thurber and Hanson [13] demonstrated temperature imaging using acetone-PLIF. The imaging of temperatures was derived from single and dual wavelength excitation techniques. In a single wavelength excitation, the flow is excited at a particular wavelength, and the fluorescence intensities are collected within the full spectrum. The collected intensities carry information regarding temperature,

concentration, static pressure, and laser energy. For an isobaric experiment with uniform concentration and laser energy, at a particular excitation wavelength, the collected fluorescence intensity is related to the fluid temperature [13].

Flow pressure and laser energy are two factors that can be controlled during an experiment. It is almost impossible to keep the seeding concentration uniform. To overcome this challenge, Thurber et al. [12, 14, and 15] introduced the dual wavelength excitation strategy to remove the concentration dependency of the fluorescence. Ratioing of fluorescence intensities resulting from exciting the tracer at two different wavelengths cancels the concentration impacts. For the dual wavelength excitation method, intensities are collected at two different wavelengths, simultaneously. This strategy solves the concentration dependency issue. However, providing two different wavelengths would bring more complexity to the experiment.

Kakuho et al. [16] measured the temperature distribution using two types of tracers, 3-pentanone and triethylamine, at a single excitation wavelength. Two tracers fluoresce within two independent spectrum ranges. Fluorescence corresponding to each tracer carry particular information about temperature and concentration dependency of the tracers. Although this method removes the effect of concentration dependency, using two tracers would add some difficulties into the diagnostics. Koban et al. [17] took advantage of the toluene spectroscopic properties and alleviated the challenges related to the concentration dependency effects for temperature applications. Toluene fluorescence consists of two spectrum ranges: temperature dependent and temperature independent. Toluene exhibits a red shift spectrum by increasing the temperature [17]. Particular optical lenses are used to filter the toluene fluorescence and separate each of the mentioned spectra. The fluorescence intensities of both spectra are a function of concentration, but only the red shift spectrum carries information about temperature. Ratioing these spectrum results in removing the effect of concentration.

LIF Equation

The fluorescence signal is related to specific tracer characteristics such as concentration and temperature [18]. The fluorescence signal, S_f (in units of photons), was developed by Thurber [12] as seen in Equation 1:

$$S_f = \frac{E}{hc/\lambda} \eta_{tol} \sigma(T) \int F_i(\lambda) \phi(\lambda, T) n_i(\lambda) d\lambda \tag{1}$$

Absorption cross section (σ) and fluorescence quantum yield or FQY (ϕ) are two photo-physical features for LIF measurements that describe the probability of a molecule absorbing and emitting photons, respectively [19]. These two parameters are functions of temperature, pressure, and wavelength [20]. These two features play important roles within selecting an appropriate tracer for a PLIF experiment. At a given excitation wavelength and isobaric condition, the fluorescence signal is expressed as Equation 2. Hence, the fluorescence signal is only function of temperature, concentration, and optical system response.

$$S_f \propto \sigma(T) \int F_i(\lambda) \phi(\lambda, T) n_i(\lambda) d\lambda \tag{2}$$

PLIF Tracer Selection

Selecting a proper tracer is an important factor when using a LIF technique. Several tracers have been used based on flowfield features and applications [5]. Examples include OH, NO, acetone, 3-pentanone, and toluene. Each tracer has to retain the following

specifications to be applied in a LIF diagnostic. The tracer must possess a vigorous non-resonant fluorescence spectrum within a UV excitation wavelength. The absorption spectrum needs to be accessible using a high power light source. Also, it is preferable that the tracer has a high vapor pressure at room temperature to make the seeding process more convenient [19]. Three tracers, which meet the needed requirements, are acetone, 3-pentanone, and toluene.

Acetone has been used in a variety of applications from flow visualization to concentration measurements within gaseous flow near room temperature and atmospheric pressure [21]. 3-pentanone has been mostly used in combustion systems. Toluene has been recently applied in a variety of fields such as thermal stratification, concentration measurement, and flow visualization [20]. Due to its spectroscopic and fluorescence characteristics, toluene separates itself as an ideal tracer for quantitative temperature measurement applications. Toluene has the best temperature sensitivity in comparison with the other tracers (80% increase in fluorescence intensity with 100K increase in temperature).

It is important to note that a specific excitation approach is required for each tracer because the excitation wavelength influences the fluorescence emission. There are three standard laser excitations choices: 248nm, 266nm, and 308nm. Toluene has higher FQY and absorption cross section in comparison with the other tracers considered. Therefore, toluene is chosen in this study as the tracer for quantitative temperature field measurements.

Two-Color Thermometry Method

As shown previously, the fluorescence signal is a function of pressure, temperature, and tracer concentration. It is impossible to keep the tracer concentration constant through the entire fluid domain. As a result, the toluene fluorescence intensity depends on both temperature and tracer concentration. Therefore, a need exists to control the tracer concentration and remove the effect of its concentration for thermometry measurements.

A valuable spectroscopic property of toluene, strong temperature dependency of its fluorescence signal, nominates this tracer for a quantitative thermometry. Toluene fluorescence shows a red shift by increasing the temperature. The general fluorescence behavior of toluene consists of two regions: (a) the spectra peak shows a shift by increasing the temperature and (b) no shift is observed by increasing the temperature. In the other words, near the wavelength of 280 nm, the fluorescence spectra are insensitive to temperature (blue spectra) and at wavelengths greater than 305 nm, the fluorescence spectra are sensitive to temperature (red spectra).

The emission intensity, of toluene, in both regions (280 nm and 305 nm) is dependent on the tracer concentration. As the emission intensity is similarly effected at both wavelengths, this effect can be removed by dividing the emission signals measured at both wavelengths. With the effect of concentration removed, the only remaining factor effecting the fluorescence intensity of the toluene is the temperature of these tracer particles. To obtain the fluorescence intensity of the toluene at two different wavelengths, two optical filters are required to pass separate fluorescence wavelengths. The fluorescence signal passing through each filter S_{f-Red} and S_{f-Blue} can be expressed using Eqn. 1. The ratio of these two intensities, Equation 3, is only a function of temperature and optical system response.

$$\frac{S_{f-\text{Re}d}}{S_{f-\text{Blue}}} = \frac{\int F_{i-\text{Re}d}(\lambda)\phi(\lambda,T)n_{i-\text{Re}d}(\lambda)d\lambda}{\int F_{i-\text{Blue}}(\lambda)\phi(\lambda,T)n_{i-\text{Rbue}}(\lambda)d\lambda}$$
(3)

The optical system response comes from variation of the image's brightness and camera uniformity. In order to remove this effect from the integral, the intensity ratios are normalized by the intensity ratio at a known temperature (Equation 4).

$$\frac{S_{f-\text{Re}d}(T)/S_{f-\text{Re}d}(298)}{S_{f-\text{Blue}}(T)/S_{f-\text{Blue}}(298)} = \frac{\int_{f-\text{Blue}} F_{i-\text{Re}d}(\lambda)\phi(\lambda,T)d\lambda/\int_{f-\text{Re}d} F_{i-\text{Re}d}(\lambda)\phi(\lambda,298)d\lambda}{\int_{f-\text{Blue}} F_{i-\text{Blue}}(\lambda)\phi(\lambda,T)d\lambda/\int_{f-\text{Blue}} F_{i-\text{Blue}}(\lambda)\phi(\lambda,298)d\lambda}$$
(4)

PLIF, as an optical diagnostic technique, relies on the spectroscopy properties of the tracer. The tracer selection plays a crucial role in PLIF experiments. The purpose of this investigation is to develop a non-intrusive method to study the flow field temperature. Therefore, the fluorescence intensity must have a great sensitivity to the flow temperature gradient. Spectroscopic properties of toluene make it a great candidate for this study.

A variety of tools exists to measure surface temperatures, and in recent years, optical techniques have quickly developed to provide detailed surface temperature distributions. In addition, optical methods have rapidly advanced to provide detailed, quantitative information across flowfields. To complement the tools commonly used in laboratory investigations, it is desirable to have a method capable of providing detailed temperature distributions within a fluid. The objective of this investigation is to develop and implement a technique to obtain two-dimensional temperature distributions of a fluid operating near room temperature. To demonstrate the method, a heated, free jet is used. The full calibration and testing procedures are presented along with the details of the data reduction process. Upon benchmarking of the process, the method can be applied to more complex flow fields.

PLIF EXPERIMENTAL FACILITY

In PLIF imaging, flow is seeded with a fluorescing material known as a tracer (toluene for this investigation). A laser beam spreads into a laser sheet (using optics) and excites a two dimensional region of the flow. The laser wavelength is proportional to the resonant transition of the tracer. Molecules within this region move to a higher energy level resulting from absorption of the laser's energy. The excited molecules then return to an equilibrium level of energy by fluorescing (emitting energy at a longer wavelength). The intensities corresponding to the fluorescence are collected using optical detectors such as CCD cameras and lenses. Two color thermometry, single excitation wavelength (266nm), and single camera image detection are established in this work for quantitative temperature measurements. This study focuses on the development of an experimental arrangement of toluene-based PLIF, the data collection process, and the data reduction procedure.

Facility Overview

All experimentation was performed in the Convective Heat Transfer Laboratory (CHTL) at Baylor University. The flow line is made of aluminum tubing with a round cross section, 0.0254 m in diameter. An inline heater is used to generate elevated temperature flow conditions required for the PLIF method development. The entire line is wrapped in fiberglass insulation to reduce heat loss from the test section. Standard T-type thermocouples are placed at desirable locations to monitor the flow temperature. The thermocouple output is monitored and recorded using LabVIEW

software from National Instruments. The output temperatures are recorded every second and written to a data file.

A laser system is used as a primary excitation source for PLIF diagnostics. The detection system consists of a CCD camera, optical lenses, and data collection computer. The experimental setup was designed and built for the purpose of PLIF diagnostic development and validation. **Figure 1** shows the schematic of the general PLIF setup used for this study.

Laser System

The laser is one of the crucial components for the PLIF method. A Neodymium doped Yttrium Aluminum Garnet (Nd:YAG) laser from Litron Laser is used for this study. The excitation wavelength selected for this study, due to the fluorescence features of toluene, is 266 nm, and this wavelength is producible using an Nd:YAG laser. A laser beam is spread into a thin plane using a cylindrical lens with $f = -20\,$ mm. In order to create an instantaneous visualization, a pulse width about 100 ns is used for the laser. The laser energy output is in the range of 40 to $120\,$ mJ / cm².

Optical Detection System

The fluorescence signals are collected by an optical system that consists of an intensified CCD camera, equipped with an Intensify Relay Optics (IRO) from LaVision. The camera has a 172×260 pixel CCD array with 6.45 μ m pixel size and it is 4×4 hardware binned. The camera exposure time is set at 6000 μ s. The combination of a CCD camera and IRO increases the sensitivity of the system to measure the ultraviolet fluorescence signal range. The optical system is equipped with an IRO controller that allows for the adjustment of the timing of the camera and laser. The optical system is placed at a right angle to the laser sheet.

A UV lens from Nikkor-UV is used to focus the images on the camera. The lens is set at its lowest f-number to achieve the highest photon efficiency. Two filters are used for two different wavelength ranges for the toluene emission spectrum. The first wavelength range is temperature independent while the second is temperature dependent. The temperature independent filter (blue detector) and the temperature dependent filter (red detector) passes 285 nm and 320 nm wavelengths, respectively. Both the 285 nm and 320 nm optical filters are narrow bandpass filters. For the "red" detector, maximum transmission efficiency is achieved at $285 \pm 2 \text{ nm}$ (with a full width-half max of $10 \pm 2 \text{ nm}$). The 320 nm fluorescence passes through a separate filter with a peak transmission efficiency at 320 ± 2 nm. With a full width, half max range of 12 ± 2 nm, the fluorescence passing through the "red" filter does not overlap that of the "blue" filter. The ratio of these two signals gives the temperature information without dependence on tracer concentration.

Toluene Seeding System

A toluene seeding system, made out of a 0.0762 m diameter aluminum pipe and sealed with two flanges at each end, disperses the toluene into the flow line. This system works based on the bubbling principle and provides a saturated air and toluene gas mixture. Two rotameters are used to monitor the flow rate of the air through the heater and bubbling system. Air enters the bubbling system through a 0.0127m inlet pipe and provides a saturated air and toluene gas mixture. The mixture leaves the bubbling system through a 0.0127 m outlet pipe and meets the heated air at a T-junction. Two check valves are installed after the outlets of the heater and the bubbling system to avoid a reverse flow.

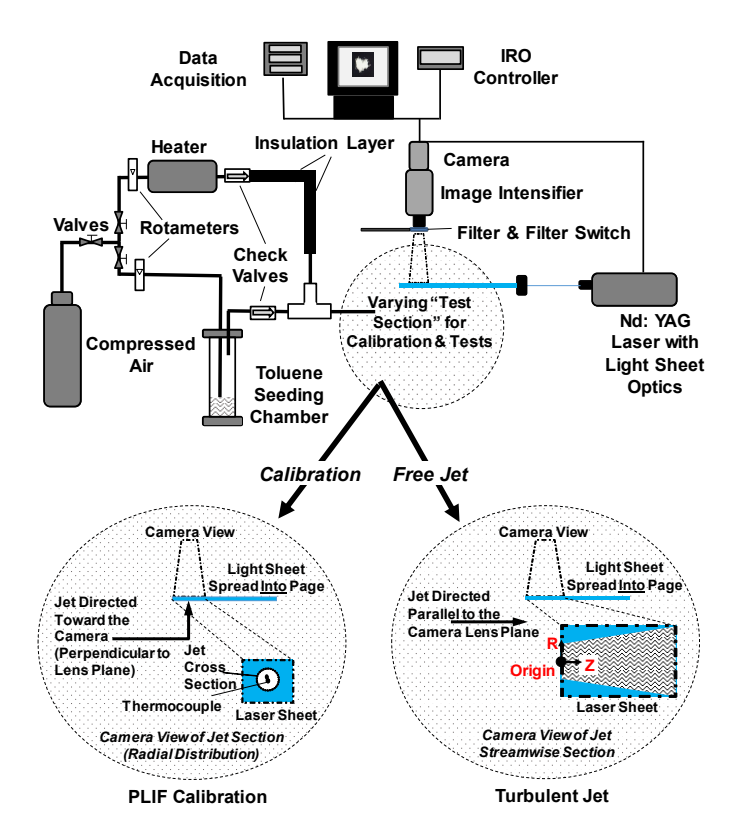


Figure 1: General PLIF Setup

Data Collection Procedure

The PLIF experimental procedure consists of three main image recording steps: background images, reference images, and air/toluene images at different temperatures. For each step, two sets of 500 images are recorded: temperature dependent (using red filter) and temperature independent (using blue filter). Background images are captured while the laser is on and there is only airflow in the system, because it is desired to record the optical noise that is created by the surrounding light. Reference images are taken while the mixture of air and toluene is flowed in the system at room temperature (297 K) and the laser is on. After the system reaches the desirable steady-state condition, the air/toluene images are recorded while the laser in on. Davis 8.3 software from LaVision is used to record the raw images. For each step, flow and ambient temperatures, gauge pressure, and flowrate are monitored and recorded. Images are exported from Davis in the tagged image file (TIF) format then post processed using in-house MATLAB code.

PLIF CALIBRATION PROCEDURE

PLIF is a non-intrusive method that quantitatively measures the flow field parameters. As previously mentioned, the scope of this investigation is to develop PLIF to study the temperature field within a fluid. The fluorescence intensity of the tracer particles is captured within a PLIF experiment. A calibration must be completed to determine the relation between the fluorescence intensity and the fluid temperature.

Calibration Setup

The first step of this study is to develop an empirical relationship between the temperature of the tracer and its florescence intensity. Figure 1 shows the schematic of a calibration setup for the PLIF measurement, and an overview of the flow line was presented in the previous section. The toluene fluorescence

wavelength is within the range of 270 - 370 nm. It requires a specific window to pass the mentioned wavelength range without changing the fluorescence properties. Since this method is highly dependent on the fluorescence intensity, using any glass window to perform the calibration is avoided. The temperature profile is uniform throughout the central region of a steady state jet cross section. Therefore, the calibration experiment is carried out through a cross section of a free jet.

Flow with a Reynolds number of approximately 10,000, based on the inner tube diameter, is used for the calibration. The air supplied from a compressor is divided into two separate streams: 80% of the flow goes to the heater and the rest goes to the seeding system. A valve and a rotameter control the flow in each line. Standard T-type thermocouples are placed at the inlet and outlet of the heater and within the central region of the jet cross section to record the air temperatures. The calibration process is performed at a variety of temperatures between room temperature and 400 K. For each measurement, the flow first passes only through the heater to reach the desired temperature at the exit of the tube. When the system reaches the steady state condition (no changes in temperature), toluene is introduced into the flow line through the seeding system. The heated and seeded flow meet at a T-junction. In order to provide a uniform mixture of toluene and air, an insert of twisted aluminum tape is placed in the tube. A 0.0127 m diameter aluminum tube with a length of 0.254 m is used to produce a fully developed flow for calibration purposes. The 0.0127 m diameter tube is connected to the main flow line tubing using a reducer fitting. A 90-degree pipe elbow is used to provide a cross section perpendicular to the optical system. The camera is equipped with a filter switch, which can remotely change the filter that is required for the PLIF experiment.

Calibration-Image Processing

The fluorescence intensity is a function of parameters such as temperature, pressure, tracer concentration, and laser energy. In a general PLIF experiment, it is possible to control some factors such as temperature, pressure, and laser energy. However, it is almost impossible to control the concentration of the tracer. As a result, there is a need to apply the two-color thermometry to remove the effect of concentration. The procedure towards this method is illustrated for the purpose of developing an empirical relation between the temperature and toluene fluorescence intensity.

The PLIF experimental procedure consists of three main image recording stages: background images, air/toluene images at a reference temperature (known as reference images), and air/toluene images at different temperatures. For each stage, two sets of 500 images are recorded: temperature dependent (using red filter) and temperature independent (using blue filter). Red and blue filters pass 320 nm and 285 nm wavelength, respectively. Since one camera is used for this study, it is not possible to capture both types of images simultaneously. Temperature dependent data are first taken using the red filter, then the filter is switched to the blue filter using the filter switch. The filter switch is controlled remotely by the same computer that is used for data acquisition.

Images are captured when the system reaches the steady state condition at a desirable temperature. For background images, the laser is illuminating the jet cross section; however, the flow is not seeded (no toluene in the flow). The purpose of capturing the background images is to record the optical noise that is created by the surrounding light. Background images are captured at each

temperature. When capturing the background images for both filters is complete, the toluene is spread into the flow line through the seeding system. The seeding system uses the air at ambient temperature; therefore, the temperature at the jet cross section is closely monitored and recorded to assure the system is working under the steady state condition. After the system reaches the uniform desirable temperature, the air/toluene images are recorded while the laser is illuminating the cross section. Reference images are air/toluene images taken while the mixture of air and toluene flows in the system at room temperature (297 K). Davis 8.3 software from LaVision is used to record the raw images. The images are exported from Davis in the tagged image file (TIF) format then post processed using in-house MATLAB code. The procedure is repeated for a variety of temperatures between room temperature and 400 K.

The image processing includes the following steps: background subtraction, time averaging, two-color thermometry, and normalizing the fluorescence intensity. The offset from camera noises and surrounding light is removed by subtracting the background intensity. For this purpose, 500 background images are averaged and then the averaged background image is subtracted from each single PLIF image. At this time, the surrounding noise is eliminated from the single PLIF images and they are ready to be time averaged.

Many pixels do not capture fluorescing tracer particles. The MATLAB code is written in a way that it includes the pixels with fluorescence intensity greater than zero for calculating the average. The two-color method is applied on the time averaged results; red filter intensities divided by blue filter intensities. The ratio eliminates the effect of concentration. Finally, the two-colored intensities are normalized by the two colored results at the reference temperature. The primary reason for normalizing is to reduce effects of inconsistencies in spatial illumination and camera sensitivity. A flow chart providing the post processing procedure is shown in Figure 2. Insets are used to show sample intensity distributions for each step in the process. Examples of calibration images (radial profile of free jet) are provided for every step in the Free jet images (full streamwise distributions) are process. provided for the latter stages of the data reduction process. The procedure is repeated for images at a variety of temperatures between room temperature and 400 K with the step size of 25 K.

In order to apply this method to measure the fluid temperature, the relation between the fluorescence intensity and the fluid temperature must be determined. Therefore, a 10×10 pixel frame is created at the center area of the jet cross section for each temperature (box shown in the center of the jet for the "Normalized Intensity Ratio @ Given Temperatures, Fig. 2). Normalized intensity ratios (Equation 5) within the frame are averaged and recorded for each temperature. The normalized temperature is fitted as a function of normalized fluorescence signal ratio I_N using the method of least squares regression with a 95% confidence interval. This function will then be applied to assign temperatures corresponding to each pixel for the measured PLIF ratio image. Figure 3 presents the data points that are used in the calibration process as well as the calibration curve. Six sets of data, each including five data points, were collected at different times, and used to create the calibration curve. The fitted equation for the linear method that describes the relation between the normalized temperature and normalized fluorescence signal ratio

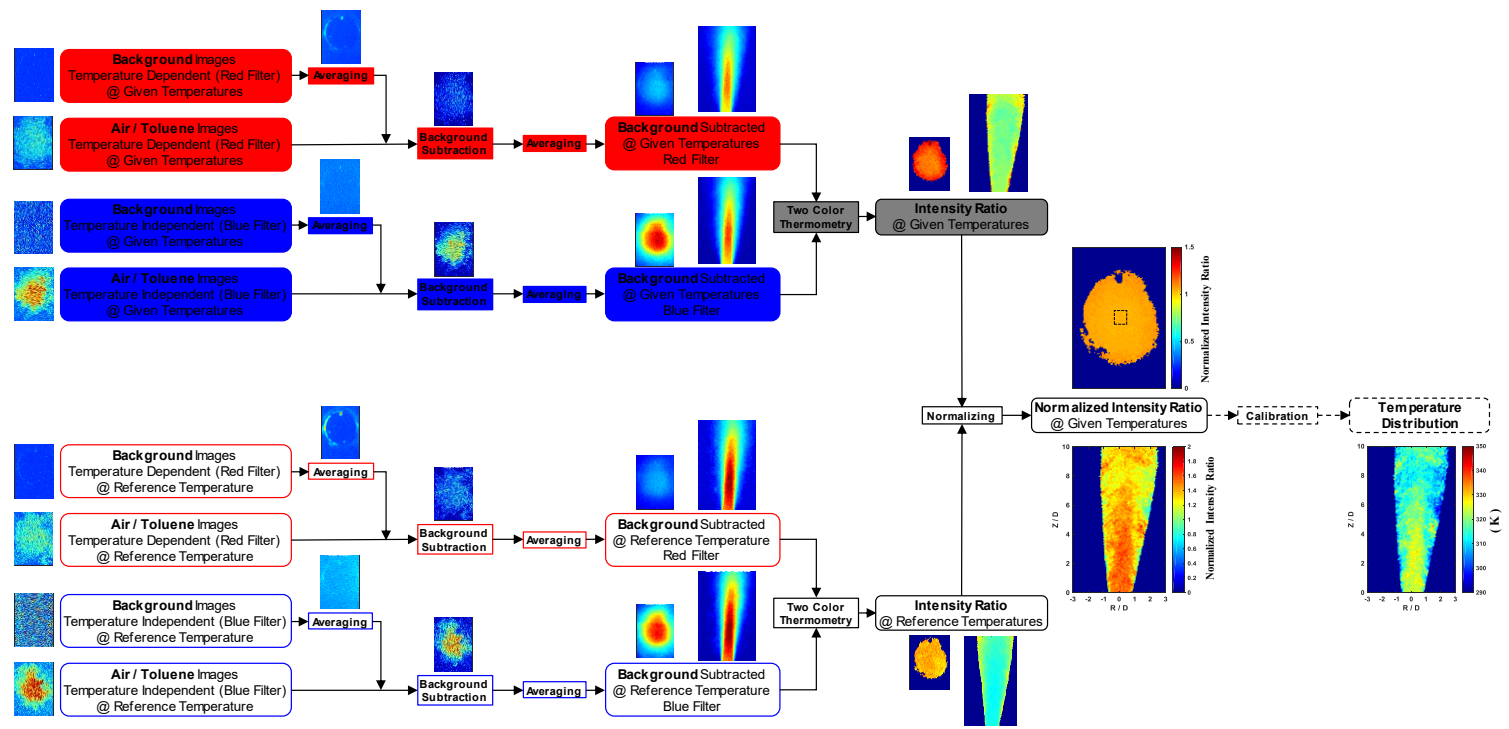


Figure 2: PLIF Data Reduction Procedure
(Including Sample Intensity, Intensity Ratio, and Temperature Distributions:
Calibration Reference Temperature = 297 K, Calibration Temperature = 305 K)

$$I_{N} = \left(\frac{I_{Red} - I_{Back-Red}}{I_{Blue} - I_{Back-Blue}}\right)_{T} / \left(\frac{I_{Red} - I_{Back-Red}}{I_{Blue} - I_{Back-Blue}}\right)_{T_{ref}}$$
(5)

Repeatability of Calibration Experiment

For this study, the calibration is conducted under specific experimental conditions. The flow Reynolds number is approximately 10,000, the seeding setup is arranged in a way that 20% of the flow goes to the seeder and the rest goes to the heater, and 500 images are captured for each filter. In order to verify the repeatability of the calibration data, impacts of the three factors on calibration data are investigated: different Reynolds numbers, seeding setups, and number of images.

Two sets of calibration experiments are conducted at Re \approx 5,000 and Re \approx 15,000 and the results are compared with the data used for calibration curve at Re \approx 10,000. As can been seen in Fig. 3, data from varying the Reynolds number falls within the 95% confidence interval.

Three different seeding setups are used to validate the repeatability of the two-color method at higher toluene concentrations. The setup arrangements are summarized in Table 1, and the results are compared in Fig. 3. Seeding setup I is used to create the calibration data. Finally, the impact of number if images on the calibration data is studied. For this purpose, calibration experiments were conducted on four different days. Different numbers of images, with the range of 100 to 400, were captured on each day. Again, the calibration curve represents the calibration data over a wide range of seeding and flow conditions. The range of all data is captured within $\pm 6\%$ of the calibration equation. As mentioned previously, for calibration post processing, a small area within center of the jet is used to collect the intensity information. However, for other applications that require a larger area, more images may be required.

Table 1: Toluene Seeding Setup Arrangements for PLIF Calibration

Seeding Setup	Heater Flow (%)	Seeder Flow (%)		
Seeding Setup I	80	20		
Seeding Setup II	75	25		
Seeding Setup III	50	50		

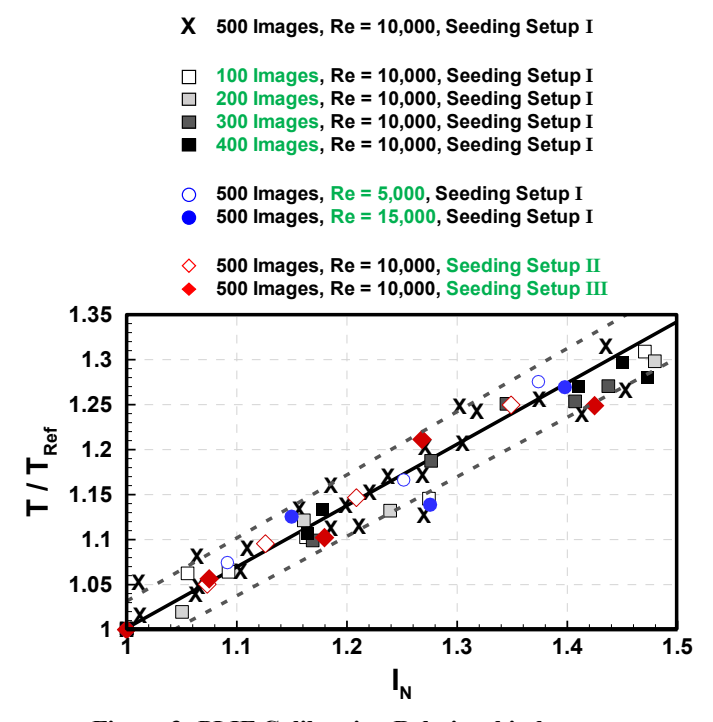


Figure 3: PLIF Calibration Relationship between Normalized Intensity and Temperature Ratios

Fluorescence Intensity Standard Deviation and Error

The PLIF temperature distribution is determined in the following steps: background subtraction, two-color method, and normalizing. The accuracy of each step contributes to the overall precision of the temperature measurement. Using the theory of propagation for a given function, the standard deviation of the function can be calculated. As shown in Fig. 3, and linear relationship exists between the measured normalized, intensity ratio and the temperature ratio. From these ratios, the fluorescence intensity of the raw images, reference images, and background images are contributing to the overall precision of the PLIF method.

The standard deviation of temperatures corresponding to the data used to create the calibration curve has been calculated. The maximum standard deviation, based on post processing of 500 images, is equal to 12.50 K at 334.87 K. The maximum relative standard deviation for this study is approximately 3.73%. Sensitivity of the standard deviation to each step varies at different temperatures. However, the calculations show that the background subtraction and two-color method have the lowest and highest contribution to the standard deviation, respectively. At a maximum standard deviation of 3.73%, the proportion of background subtraction, two color method, and normalizing steps are, namely, 16.25%, 54.12%, and 29.63%.

The standard deviation is in agreement with literature standard deviations corresponding to LIF experiments. As an example, Kearney and Reyes [22] estimated the standard deviation of 1.8% for temperature measurement in a turbulent, thermal convection study using acetone-LIF. O'Byrne et al. [23] reported a standard deviation of 4.5% in PLIF temperature measurement in laminar hypersonic flat plate flows.

In addition, standard deviations corresponding to the slope and intercept of the calibration curve have to be considered to obtain the uncertainty of the calibration tests. Since a linear least squares curve fit is made for the calibration set of data, a standard error of regression can be applied to calculate the standard deviation corresponding to the slope and intercept [24]. Using this method, the standard deviation for the slope and intercept of the calibration relationship is equal to 0.068 (9.94%) and 0.041 (12.75%), respectively. The theory of propagation can be used to combine the standard deviations of fluorescence intensities, calibration curve slope, and intercept. The overall uncertainty corresponding to calibration tests is equal to 16.59%.

The major sources of uncertainty for the PLIF calibration study could be related to camera noise, filter detectability error, laser energy, and toluene purity. Cameras create dark and shot noises. In the PLIF study, the majority of dark noise is removed through the background subtraction process. The shot noise is a result of capturing undesirable information, and impact the image resolution. Sensitivity of the standard deviation to each of the steps (background subtraction, two-color method, and normalizing) is calculated. It is found that the background subtraction step has the lowest impact on the standard deviation.

The standard deviation for the PLIF calibration has the highest sensitivity to the two-color method step. In the PLIF calculation, the intensity ratio of the temperature dependent images to temperature independent images is calculated to eliminate the effect of concentration. For this study, a single camera is used to capture the temperature dependent and temperature independent fluorescence signals. Therefore, the two types of images are not recorded simultaneously. The delay between switching the filters and capturing two types of images could create errors.

For this study, a planar laser is used to excite toluene molecules. The laser energy may change within its plane, and results in creating an uncertainty. The two-color method and normalizing can partially remove this effect. However, since two types of images (temperature dependent and independent) are recorded separately, the possibility that the laser energy varies during the data collection and its gradient affects the florescence quality. To reduce the laser energy error, the laser energy has to be monitored and adjusted during image collection using laser power meters

Toluene impurity could contribute to error production. The PLIF method works based on capturing the toluene fluorescence intensity. The toluene molecules absorb the energy of the laser and travel to a higher energy state. The excited molecules emit energy, in the form of fluorescence, while they are reaching the equilibrium state. The presence of contamination and impurities in toluene could affect the energy absorption and photon emission.

RESULTS AND DISCUSSION

This study focuses on developing a novel, non-intrusive method to measure the flow field temperature. An empirical relationship between the temperature and fluorescence intensity was developed. Now the experimental results of a PLIF application on free jets can be presented. To start, a general background behind free turbulent flows is summarized. Secondly, features of the experimentation for the free jets are outlined. Finally, the results of PLIF experimentation are provided.

Turbulent Jets

Free turbulence flows are shear streams with high Reynolds number flow through an open environment fluid. A free jet is formed when a flow leaves a nozzle or orifice and is discharged into a flow with a negligible velocity. Free jet flows are widely used in many engineering applications such as drying, cooling, propulsion, and air conditioning systems. The jets are flows with a specific momentum that spread into another fluid (usually a stagnant fluid).

Transition from laminar to turbulence for round jets occurs at Reynolds numbers on the low side of 102 [25] and become fully turbulent for Re > 2,000 [26]. Heat and mass transfer enhancement are special characteristics of the turbulent jets. Fellouah et al. [27] investigated the effects of jet Reynolds number at different distances downstream from the jet exit (0 < Z / D < 25) using a hot-wire technique to determine the differences in mean velocity and turbulence intensity distribution. The Reynolds numbers used for the experiment were 6,000, 10,000, and 30,000. It was shown that the impact of Reynolds number varies at different regions of the jet. The effect of the Reynolds number is more significant within the shear layer region. It was also found that by increasing the Reynolds number, the thickness of the boundary layer at the jet exit decreases and the length of the potential core increases.

Researchers have also used flow visualization techniques to characterize the behavior of free jets. Popiel and Trass [28] visualized the behavior of natural free jets, for two Reynolds numbers of 10,000 and 20,000, at regions near the nozzle exit using the smoke-wire flow visualization technique. It was found that the creation of vortices near the nozzle exit disturbs the boundary layer and leads to the elongation of the jet core. Kwon and Seo [29] used the particle image velocimetry (PIV) method to obtain the jet mean velocity and study the impact of Reynolds number on development of flow regions within free jets. It was found that the turbulent flow spreading rates gradually decreased by increasing the Reynold number. Dimotakis et al. [30] used laser

induced fluorescence and particle streak velocity methods to obtain some physical insights into the structure and dynamics of turbulent jets. While recent researchers have used PIV methods to study the flow field. There is still a need to investigate the thermal flow fields, especially within the boundary layers where obtaining measurements is complicated.

Free Jet Facility

The flow path of air for the free jet is very similar to the calibration setup. The jet cross section was used for the calibration purposes. For the free jet study, a streamwise cut at the center of the jet is desirable. In order to produce a free jet, a 0.0127 m diameter aluminum tube is connected to the PLIF flow line using the appropriate fitting. The tube length and jet diameter are 0.254 m and 0.0127 m, respectively. The ratio of the jet length – to – diameter is equal to 20. The entrance length for turbulent flow is approximately equal to ten pipe dimeters [31]; for this study, the tube is long enough to produce fully developed flow.

A schematic of the free jet setup is shown in Fig. 1. The camera is placed at a distance from the jet to record the length equal to 0.127m downstream of the jet exit. The jet temperature is measured at the center of the jet at the nozzle exit, and varies between 300 K and 375 K with the step size of 25 K. Three Reynolds numbers of 5,000, 10,000, and 15,000 are used to produce turbulent free jets. The jet exit, jet streamwise cut, origin and the coordinate system used to present the free jet results are also illustrated in Fig. 1.

Experimental Procedure

The PLIF experimental procedure for free jet tests consists of three main image recording steps: background images, reference images, and air/toluene images at different experimental conditions. For each step, two sets of 500 images are recorded: temperature dependent (using red filter) and temperature independent (using blue filter). Background images are captured while the laser is on and there is only airflow in the system (no tracer particles). Reference images are taken while the mixture of air and toluene is flowing in the system at room temperature (297 K) and the laser is on. Background images are taken for each filter at each temperature. There are two thermocouples located at the center of the jet at the nozzle exit. The temperature is closely monitored. After the jet reaches the steady state condition (constant temperature at the tube outlet), the toluene is introduced to the flow line from the seeding system. It is important to monitor the total flowrate to maintain the same Reynolds number. The air/toluene images are recorded while the laser is on. Davis 8.3 software from LaVision is used to record the raw images. Images are exported from Davis in the tagged image file (TIF) format then post processed using an in-house MATLAB code.

Data Reduction

The data reduction for the free jet experiments is very similar to the calibration data reduction. However, in order to reduce the noise, the two-color method process is slightly different for the free jet experiment. For the calibration image processing, a very small area located at the center of the jet cross section was desirable to collect the intensity information. However, for the free jet tests, the whole jet is studied for the PLIF validation. As was mentioned in the description of the calibration procedure, there are pixels that do not capture fluorescing tracer particles. Including these pixels in the time averaging process and two-color method would lead to increased uncertainty of the experiment as well as including additional noise.

For this investigation, the 500 single raw images are background subtracted and time averaged. It is important to note that only pixels that carry an intensity magnitude greater than zero are considered in the time averaging process. A distribution of the number of images that carry desirable intensities (intensity greater than zero) for the time averaged images are created. This distribution, known as count, is used later as a threshold for the two-color method procedure. The count distribution presents how many images at each pixel are used for the time average process. In the other words, it shows the distribution of the number of images that capture a fluorescence tracer particle at each pixel. Figure 2 includes samples of the time averaged images for temperature dependent (red filter) and temperature independent (blue filter) signals.

In order to apply the two-color method, propagation of the temperature dependent and the temperature independent count is calculated as

Combined Count =
$$= \sqrt{(Temperature Dependent Count)^2 + (Temperature Independent Count)^2}$$
(6)

From the combined count distribution, the median value of the combined count is extracted and used as a threshold for the two-color method. Pixels of the time averaged images that carry a count greater than the median value of the combined count are used in the two-color method. The same procedure is repeated on the free jets at higher temperatures. Figure 2 includes the post processing results on the free jet at $T=324.60~\mathrm{K}$ and Re=10,000.

The room temperature is the reference temperature for this experiment. The intensity ratio at the reference temperature is used in the normalizing procedure. The normalized image is the result of dividing the intensity ratio distribution at a given temperature by the intensity ratio obtained at the reference temperature. The normalizing procedure reduces the effect of inconsistencies in spatial illumination and camera sensitivity. In order to calculate the temperature distribution, the PLIF calibration correlation is applied to the normalized intensity ratio. The temperature distribution for $T=324.6~\mathrm{K}$ at Re=10,000 is shown as the last step in Fig. 2.

For the free jet experiments, 500 images are recorded for each test. The impact of number of images on the experiments are studied to confirm that 500 images are an adequate number. For this purpose, a comparison was conducted among a variety of number of images that are used for the post processing. **Figure 4** presents the impact of the number of images on the radial temperature distribution at downstream location of Z/D=5 for free jets at T=324.60 K and Re=10,000. As is seen, the data corresponding to 50 images are dispersed. As the number of images is increased, the data consistency improves. The impact of the number of images on the PLIF results are studied for all cases. At a 95% level of confidence, the data provide sufficient evidence that using more than 350 images does not affect the results.

PLIF Free Jet Results

For this study, free jet tests are created at nozzle temperatures ranging from 300 K to 375 K with the step size of 25 K. From these cases, the impact of jet Reynolds number on thermal development is investigated to validate the PLIF technique. The test cases are summarized in Table 2.

Detailed temperature distributions for cases with $Re=10,\!000$ are presented in **Figure 5**. The temperatures at the jet nozzle exit, recorded by thermocouples, are provided above the distribution. The PLIF experimental results near the jet exit closely agree with the thermocouple data. The relative error of the temperature near

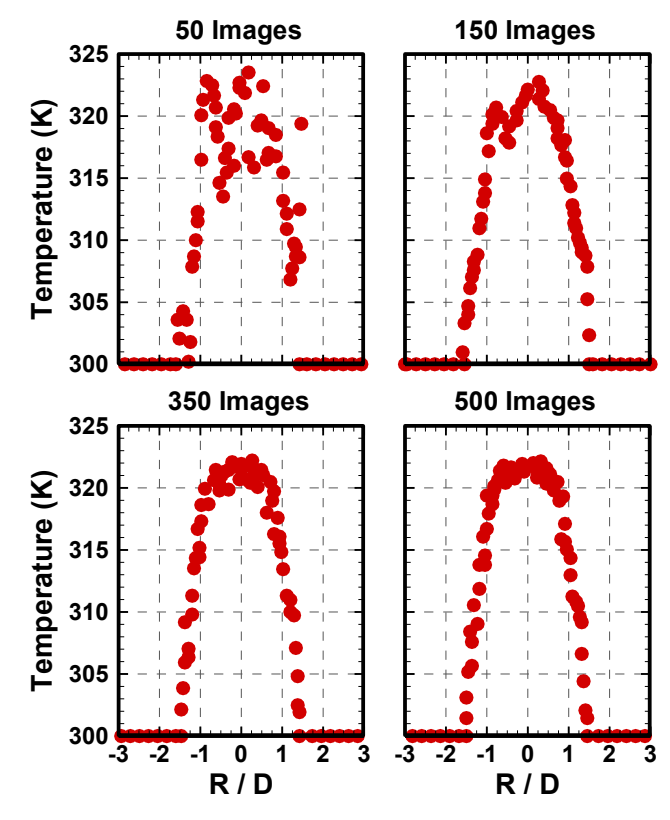


Figure 4: Influence of the Number of Images on the Jet Temperature Profile (Z/D = 5, $T_{Jet} = 324.60$ K, Re = 10,000)

Table 2: Free Jet Test Cases

Jet Reynolds Number	Outlet Temperature (K)
5,000	300, 325, 350, 375
10,000	300, 325, 350, 375
15,000	300, 325, 350, 375

the jet exit, $|T_{PLIF} - T_{TC}| / T_{TC}$, for all cases are less than 6%. The standard deviation analysis for full jets is performed on the case with Re = 10,000. The relative uncertainties for the free jets at jet nozzle temperatures equal to 300.30 K, 324.60 K, 347.70 K, and 372.40 K are equal to 0.98%, 1.58%, 3.18%, and 2.76%, respectively. The uncertainties calculated for free jets agree with the calibration uncertainties described previously. The free jet experiments were conducted on different days. Thus, the reference temperature (room temperature) is not constant for all cases. The impact of this change is mostly eliminated through the normalizing process.

A dimensionless temperature, θ , is defined (Equation 7) to maintain the consistency in comparing the results of the PLIF free jet cases. The reference temperatures (room temperatures) for this calculation are provided from thermocouple data; the jet (nozzle outlet) temperatures are directly extracted from the PLIF results. The dimensionless temperature, θ , varies between the range of zero and one. The θ equal to zero means that the local temperature is equal to the reference temperature, and the θ equal to one means that the local temperature is equal to the jet temperature at the nozzle exit. When the turbulent flow exits the nozzle, a mixing occurs between the jet core and ambient flow. The dimensionless temperature illustrates the extent of the mixing between the jet core and the ambient flow. For the areas with θ approaching unity, there is no mixing effect and jet is maintaining the nozzle exit

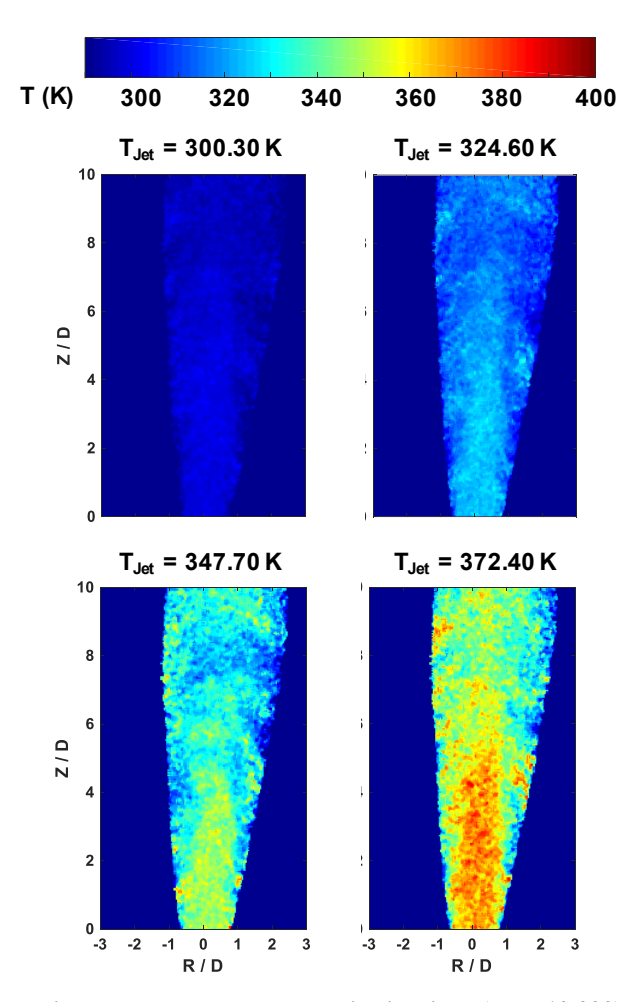


Figure 5: Jet Temperature Distributions (Re = 10,000)

temperature. The mixing effect is at its highest for areas with θ equal to zero when jet reaches the room temperature.

$$\theta = \frac{T - T_{Ref}}{T_{Jet} - T_{Ref}} \tag{7}$$

Detailed, dimensionless temperature distributions for cases with Re = 10.000 are presented in Figure 6. The θ distributions show similar magnitudes independent of the jet temperature. This figure also provides information about the jet core region. The jets retain the nozzle exit temperature in their potential cores. Moreover, the potential cores remain intact until approximately the same distance from the jet outlet $Z/D \approx 5$ for all four cases, which is expected to be observed for cases with the same Reynolds number. For the momentum potential cores, it is expected to observe the uniform velocity until approximately seven diameters downstream from the jet outlet [32, 33]. Available experimental investigations on free jets have primarily focused on the jet velocity. Theory has shown the core of the turbulent, free jet is expected to remain intact until approximately 5.65 diameters downstream from the nozzle exit [25]. The thermal potential cores observed from PLIF tests only for cases with Re = 10,000 agree with the theoretical solutions.

Before exploring the effect of Reynolds number on the thermal structure of the jet, it is necessary to discuss several artifacts of the proposed PLIF technique. Although the distributions shown in Figs. 5 and 6 represent "time averaged" temperature profiles, the distributions do not take on the notable characteristics of time averaged distributions. Each temperature

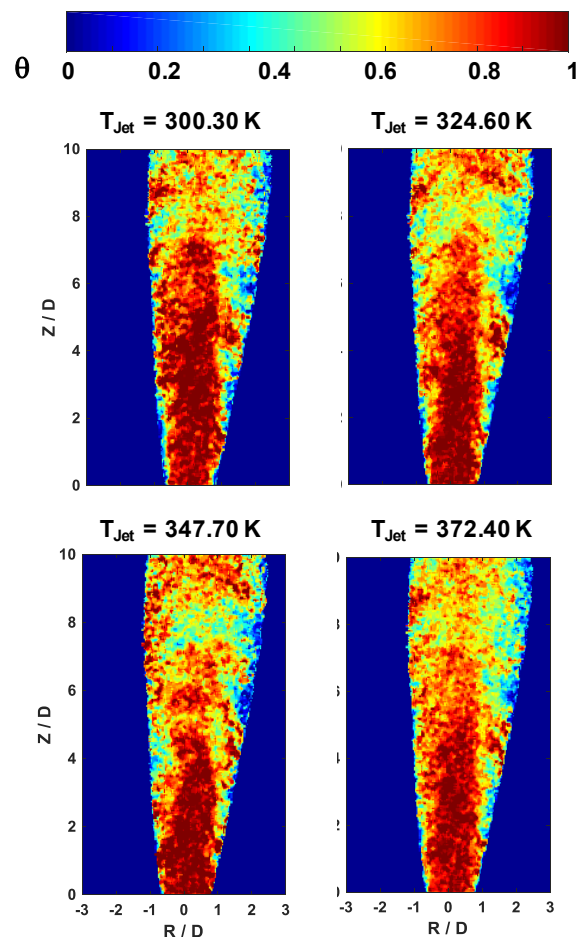


Figure 6: Dimensionless Jet Temperature Distributions (Re = 10,000)

distribution shown in Fig. 5 is the culmination of eight different image sets (each set consisting of 500 images). The small insets in Fig. 2 show typical intensity distributions obtained throughout the process. The "background subtracted" intensity distributions depict a more typical time-averaged jet structure. However, the pixel – by – pixel ratioing of these distributions introduces scatter into the distributions. Also, the magnitudes of the intensity distributions obtained using the temperature dependent and independent filters are relatively close to one another, so pixel – to – pixel variation can appear amplified.

Another distinct feature of the distributions appears along the outer edges of the jet. Again, looking at the intensity distributions shown in Fig. 2, the gradual decrease of the intensity from the seeded jet to the unseeded quiescent air is captured. temperature distributions shown in Figs. 5 and 6 show a much more abrupt change from the jet to the stagnant surrounding air. The outer boundaries of the jet are defined based on the "threshold" from the combined count of the temperature dependent and independent intensity distributions. The threshold value has been set to increase the confidence of the primary features within the core of the jet. Reducing the number of instances occurring from the 500 images, would provide a wider signature of the jet. With more mixing occurring along the edges of the jet, a single pixel will provide an intensity for the instances when the jet fluid covers the pixel. However, when the surrounding air occupies the pixel, no intensity is measured for that instant in time. For the current study, regions of high shear are not fully portrayed due to the thresholding procedure. This is further complicated by the use of a single camera and separate image sets obtained with the two

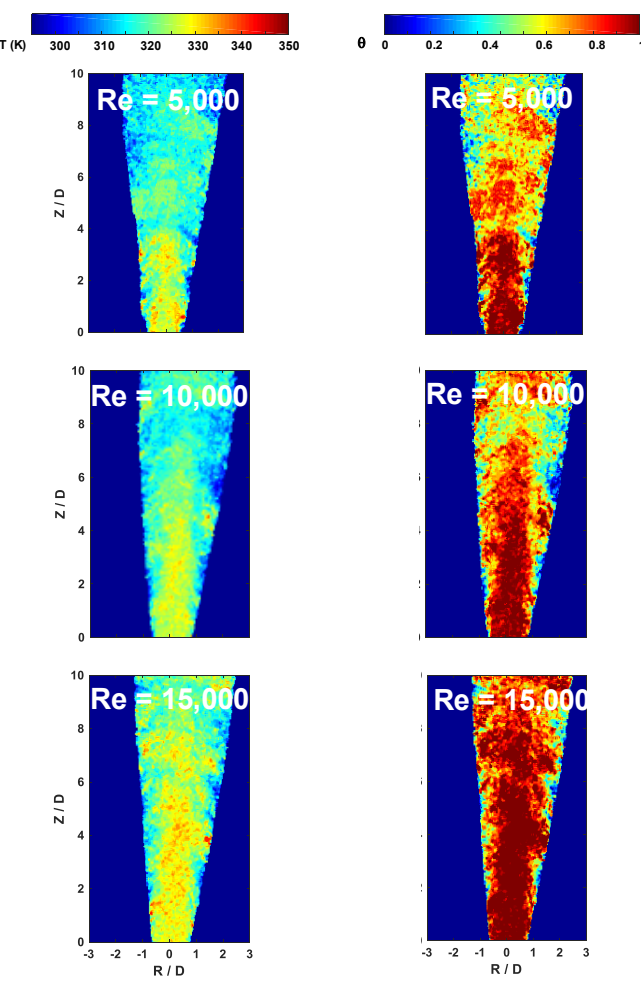


Figure 7: Effect of Reynolds Number on Free Jet Development ($T_{Jet} \approx 325~K$) – Detailed Temperature and Non-dimensional Temperature Distributions

filters. However, the core region of the jet is adequately represented by the PLIF distributions.

Revnolds Number Influence on the Jet Core

The Reynolds number has the most influence on the free jet development [29]. In this study, the impact of increasing the jet Reynolds number is investigated. Figure 7 presents the detailed distribution of the temperature and dimensionless temperature at $T_{Jet} \approx 325$ K for three different Reynolds numbers of jets. As shown in Fig. 7, an increase in the Reynolds number leads to an increase in the length of the jet potential core zone. The jets with a lower velocity (lower momentum) start exchanging the energy of the jet with the surrounding flow at a distance closer to the nozzle exit; thus, jets with lower Reynolds numbers have a shorter potential core. The impact of the Reynolds number depends on the jet region. As is seen in Fig. 7, the effect of the Reynolds number is more significant in the shear layer region where larger spread of momentum exists. The impact of the turbulent flow structure at the edge of the jet increases with increasing Reynolds number. Clearly, at higher Reynolds numbers the jet shear layer vortices exist at a further distance downstream.

Figure 7 also shows mixing layer development within free jets. Mixing layers are created between two flows with different velocities. For this study, turbulent jets spread into ambient flow with zero velocity. Figure 7 shows that mixing layers are formed near the nozzle exit lip, and grow toward the end of jet core. The

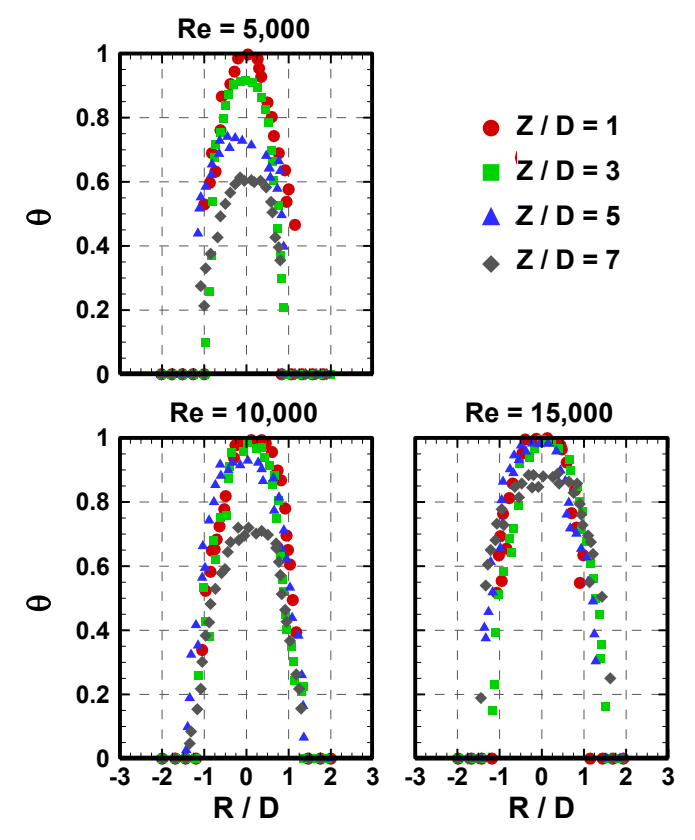


Figure 8: Radial, Non-dimensional Temperature Distributions ($T_{Jet} \approx 325 \text{ K}$)

dimensionless temperature distribution in Fig. 7 provides a better visualization between jets at different Reynolds number. As is seen, the angle of spread of the mixing layer is the same for all Reynolds numbers.

Figure 8 shows the impact of the jet Reynolds number on the radial, dimensionless temperature distribution. Data is categorized based on four distances from the jet nozzles: one, three, five, and seven diameters. As mentioned earlier, the dimensionless parameter shows the impact of mixing. In general, the dependency of the mixing on Reynolds number is more significant at locations greater than three diameters downstream of the nozzle exit. The mixing is reduced as the jet moves toward the downstream. This reduction is more significant with the Reynold number of 5,000. As the Reynolds number increases, less reduction is observed at greater distances. This can be related to the higher kinetic energy that eddies are carrying within flows with higher Reynolds number.

PLIF Comparison with Analytical Solution for a Round, Free Jet

LIF techniques have been used extensively in the past to acquire concentration gradients and more sparingly in flows at relatively high temperatures. With this study, detailed temperature distributions have been obtained within a heated jet under a variety of flow conditions and temperatures. From the detailed distributions, radial temperature profiles were extracted to quantitatively discuss the thermal development of the fee jets.

The discharge of jets into a stagnant fluid reservoir have been studied for decades. Analytical solutions for the development of both "slot" and "round" jets are readily available in literature [25]. For both types of flows, the free shear layer surrounding the jet governs the velocity and temperature profiles. Downstream of the potential core (Z/D > 5), an analytical solution can be used to describe the profile of the time-averaged, turbulent jet. Beginning with the mass and momentum equations in cylindrical coordinates,

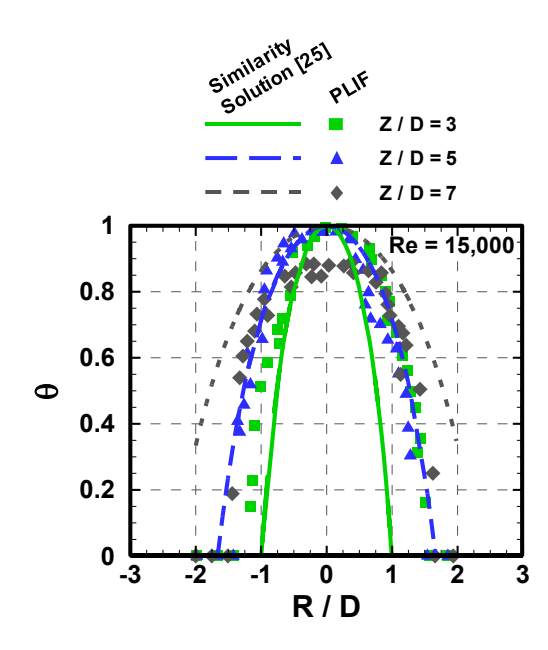


Figure 9: Comparison between Temperature Distributions Obtained using PLIF and the Similarity Solution [25] for a Round Jet ($T_{Jet} \approx 325 \text{ K}$)

a solution for the time-averaged velocity profile can be obtained using a similarity variable [25].

The present case focuses on the temperature distribution of the jet. Bejan [25] expands this discussion and provides the following equation to describe the thermal behavior of a round jet (the nomenclature has been modified to match the current study):

$$\frac{T - T_{Ref}}{T_{Jet} - T_{Ref}} = \exp\left[-\left(\frac{R}{b_t}\right)^2\right]$$
 (8)

Equation 8 directly shows the temperature distribution is dependent upon the radial location, R, within the jet. In addition, the thermal profile is changing in the streamwise direction, and this is represented by b_t . Experiments have indicated this streamwise (transversal) length scale is linearly proportional to the downstream location from the exit of the nozzle [34]. Taking into account the range of b_t and re-writing the equation in terms of the current nomenclature and coordinate system, an analytical solution for the radial temperature profile of a free jet is shown by Equation 9.

$$\frac{T - T_{Ref}}{T_{Jet} - T_{Ref}} = -\exp\left[-\left(2.5 \cdot \frac{R}{D} \cdot \frac{D}{Z}\right)^2\right] + 2 \tag{9}$$

The temperature profiles obtained using the PLIF technique are compared to those generated from the analytical, similarity solution (Eqn. 9) in **Figure 9**. As indicated by Bejan [25], this similarity solution applies to developed jets (Z/D > 5). Therefore, comparisons are included for Z/D = 3, 5, and 7 with a jet Reynolds number of Re = 15,000. As shown in the figure, the PLIF data is in good agreement with the profile proposed by the analytical solution.

CONCLUSIONS

The fluorescence behavior of substances has been used for decades to obtain measurements of pressure, temperature, or concentration. With researchers using a variety of paints to provide detailed distributions on surfaces, there is a need to complement these distributions with detailed distributions within the adjacent fluid. A variety of methods exist to characterize the flow development within the fluid. However, the ability to obtain detailed temperature distributions within a fluid is limited. Moreover, obtaining these distributions through fluids with relatively small temperature changes is an additional challenge. This work has shown that two-color, PLIF thermometry is a possible method to meet this need.

A toluene-based, two-color method of planar fluorescence measurements has been presented. The details of the experimental setup, calibration procedure, and data reduction method have been provided. After completing the calibration to obtain a relationship between the emission intensity of the toluene and the air/toluene mixture temperature, the method was used to obtain thermal maps within the center of a free jet. In its current form, the proposed method was used to obtain time-averaged temperature distributions in flows ranging from $300-375~\rm K$. The temperature profiles were obtained for jets issuing at different temperatures and varying Reynolds numbers.

The method proved its capability to capture temperature distributions under a variety of flow conditions. With the establishment of the method, it is possible to apply the technique to more complex flow fields and focus on near wall thermal boundary layer development. In addition, the acquisition of detailed temperature distributions within a fluid will be beneficial for the validation of numerical simulations.

With this novel attempt to study the thermal development of a heated, free jet, several points should be carefully considered with further implementation. In order to remove the effect of seed concentration, the ratio of images using two separate filters are needed. In the current investigation, two separate sets of 500 images were recorded at different instances in time. Utilizing two cameras simultaneously or image doubling hardware could reduce any uncertainty associated with taking the ratio of two different image sets. Furthermore, the proposed procedure includes eight different sets of images to yield the final temperature distribution.

With further implementation and increased sensitivity of image acquisition hardware, the quality of the results will continuously improve. The method has shown the potential for quantitatively assessing the thermal development of an unbounded flow. The application of the method to near-wall flows will extend the capabilities of the PLIF technique to measure temperature gradients near a surface. Not only will these gradients provide information of the thermal boundary layer development, but they will also provide a means to calculate the convective heat transfer coefficient on the surface. A variety of opportunities exists for the widespread application of the PLIF technique presented in this study. A complimentary study demonstrates the direct application of this PLIF method for the characterization of a cool jet impinging on a hot surface. In this work, the near wall temperature gradient is obtained using the PLIF method, and the surface convective heat transfer coefficients are calculated. Favorable agreement is shown between the heat transfer coefficients obtained using the PLIF method and a more traditional, convective heat transfer experiment [35].

ACKNOWLEDGEMENTS

This work has been sponsored by the National Science Foundation under award number CBET-1126371. The authors would like to thank Drs. Truell Hyde and William Jordan of Baylor University for their support of this project. In addition,

the machine work (and advice) of Mr. Ashley Orr was vital to the completion of the work.

REFERENCES

- [1] Cooper, T., Field, R., and Meyer, J., 1975. "Liquid Crystal Thermography and its Application to the Study of Convective Heat Transfer," *ASME J. Heat Transfer*, 97(3), pp. 442–450.
- [2] Lui, T. and Sullivan, J.P., 2005, *Pressure and Temperature Sensitive Paints*, Springer.
- [3] Kohse-Hoinghaus, K., 1994, "Laser Techniques for the Quantitative Detection of Reactive Intermediates in Combustion Systems," *Progress in Energy and Combustion Science*, 20(3), pp 203–279.
- [4] Hanson, R.K., Seitzman, J.M., and Paul, P.H., 1990, "Planar Laser-Fluorescence Imaging of Combustion Gases," *Applied Physics B: Lasers and Optics*, 50(6), pp. 441–454.
- [5] Schulz, C. and Sick, V., 2005, "Tracer-LIF Diagnostic: Quantitative Measurement of Fuel Concentration, Temperature and Fuel/Air Ratio in Practical Combustion Systems," *Progress in Energy and Combustion Science*, 31(1), pp 75–121.
- [6] Long, M.B., Webber, B.F. and Chang, R.K., 1979, "Instantaneous Two-Dimensional Concentration Measurements in a Jet Flow by Mie Scattering," *Applied Physics Letters*, 34(1), pp. 22–24.
- [7] Kychakoff, G., Howe, R.D., Hanson, R.K., and McDaniel, J.C., 1982, "Quantitative Visualization of Combustion Species in a Plane," *Applied Optics*, 21(18), pp. 3225–3227.
- [8] Dyer, M.J. and Crosley, D.R., 1982, "Two-Dimensional Imaging of OH Laser Induced Fluorescence in a Flame," *Optics Letters*, 7(8), pp. 382–384.
- [9] Allen, M.G. and Hanson, R.K., 1988. "Digital Imaging of Species Concentration Fields in Spray Flames," *Symposium (International) on Combustion*, 2(1), pp. 1755–1762.
- [10] McDaniel, J.C., Hiller, B., and Hanson, R.K., 1983, "Simultaneous Multiple-Point Velocity Measurements using Laser-Induced Iodine Fluorescence," *Optics Letters*, 8(1), pp. 51–53.
- [11] Seitzman, J.M., Kychakoff, G., and Hanson, R.K., 1985, "Instantaneous Temperature Field Measurements using Planar Laser-Induced Fluorescence," *Optics Letters*, 10(9), pp 439–441.
- [12] Thurber, M.C., 1999, Acetone Laser-Induced Fluorescence for Temperature and Multiparameter Imaging in Gaseous Flows, Ph.D. Dissertation, Stanford University.
- [13] Thurber, M.C. and Hanson, R.K., 2001. "Simultaneous Imaging of Temperature and Mole Fraction using Acetone Planar Laser-Induced Fluorescence," *Experiments in Fluids*, 30(1), pp. 93–101.
- [14] Thurber, M.C., Grisch, F., and Hanson, R.K., 1997, "Temperature Imaging with Single-and Dual-Wavelength Acetone Planar Laser-Induced Fluorescence," *Optics Letters*, 22(4), pp 251–253.
- [15] Thurber, M.C., Kirby, B.J., and Hanson, R.K., 1998. "Instantaneous imaging of temperature and mixture fraction with dual-wavelength acetone PLIF," *36th AIAA Aerospace Sciences Meeting and Exhibit*.
- [16] Kakuho, A., Nagamine, M., Amenomori, Y. Urushihara, T., and Itoh, T., 2006. "In-Cylinder Temperature Distribution Measurement and its Application to HCCI Combustion," SAE Paper No. 2006-01-1202.
- [17] Koban, W., Koch, J.D., Hanson, R.K., and Schulz, C., 2004. "Absorption and Fluorescence of Toluene Vapor at Elevated

- Temperatures," *Physical Chemistry Chemical Physics*, 6(11), pp. 2940–2945.
- [18] Hanson, R.K., 1988, "Combustion Diagnostics: Planar Imaging Techniques," Symposium (International) on Combustion, 21(6), pp. 1677–1680.
- [19] Yoo, J.H., 2011, Strategies for Planar Laser-Induced Fluorescence Thermometry in Shock Tube Flows, Ph.D. Dissertation, Stanford University.
- [20] Koch, J., 2005, Fuel Tracer Photophysics for Quantitative Planar Laser-Induced Fluorescence, Ph.D. Dissertation, Stanford University.
- [21] Thurber, M.C. and Hanson, R.K., 1999, "Pressure and Composition Dependences of Acetone Laser-Induced Fluorescence with Excitation at 248, 266, and 308 Nm," *Applied Physics B: Lasers and Optics*, 69(3) pp. 229-240.
- [22] Kearney, S. and Reyes, F., 2003, "Quantitative Temperature Imaging in Gas-Phase Turbulent Thermal Convection by Laser-Induced Fluorescence of Acetone," *Experiments in Fluids*, 34(1), pp. 87–97.
- [23] O'Byrne, S., Danehy, P.M., and Houwing, A.F.P., 2003, "PLIF Temperature and Velocity Distributions in Laminar Hypersonic Flat-Plate Flow," Proceedings of 12th Gordon Research Conference on Laser Diagnostics for Combustion, Oxford, United Kingdom.
- [24] Coleman, H.W. and Steele, W.G., 1999, Experimentation and Uncertainty Analysis for Engineers, 2nd ed., John Wiley & Sons. Inc.
- [25] Bejan, A., 2013, *Convection Heat Transfer*, 3rd ed., John Wiley & Sons, Inc.

- [26] List, E.J., 1982, "Turbulent Jets and Plumes," *Annual Review of Fluid Mechanics*, 14(1), pp. 189–212.
- [27] Fellouah, H., Ball, C.G., and Pollard, A., 2009, "Reynolds Number Effects within the Development Region of a Turbulent Round Free Jet," *International J. of Heat and Mass Transfer*, 52, pp. 3943–3954.
- [28] Popiel, C.O. and Trass, O., 1991, "Visualization of a Free and Impinging Round Jet," *Experimental Thermal and Fluid Science*, 4(3), pp. 253–264.
- [29] Kwon, S.J. and Seo, I.W., 2005, "Reynolds Number Effects on the Behavior of a Non-Buoyant Round Jet," *Experiments in Fluids*, 38(6), pp. 801–812.
- [30] Dimotakis, P.E., Miake-Lye, R.C., and Papantoniou, D. A., 1983, "Structure and Dynamics of Round Turbulent Jets," *The Physics of Fluids*, 26(11), pp. 3185–3192.
- [31] Cengel, Y.A. and Cimbala, J.M., 2006. Fluid Mechanics: Fundamentals and Applications, 4th ed., McGraw Hill.
- [32] Han, J.C, Dutta, S. and Ekkad, S., 2012, *Gas Turbine Heat Transfer and Cooling Technology*, 2nd ed., CRC Press.
- [33] Han, B. and Goldstein, R., 2001, "Jet-Impingement Heat Transfer in Gas Turbine Systems," *Annals of the New York Academy of Sciences*, 934(1), pp. 147–161.
- [34] Fischer, H.B., List, E.J., Koh, R.C.Y., Imberger, J., and Brooks, N.H., 1979, *Mixing in Inland and Coastal Waters*, Academic Press.
- [35] Wright, L.M. and Seitz, S., 2019, "Thermal Development of an Impinging Jet Using Planar Laser Induced Fluorescence (PLIF), ASME Paper No. GT2019-92062.